Available online at www.sciencedirect.com
SCIENCE DIRECT®
Journal of Molecular Catalysis A: Chemical 220 (2004) 189–198
JOURNAL OF MOLECULAR CATALYSIS A: CHEMICAL
www.elsevier.com/locate/molcata

A theoretical study on the cyclopropane adsorption onto the copper surfaces by density functional theory and quantum chemical molecular dynamics methods

Xiaojing Wang [a,1], Parasuraman Selvam [b], Chen Lv [a], Momoji Kubo [a,c], Akira Miyamoto [a,d,*]

[a] *Department of Applied Chemistry, Graduate School of Engineering, Tohoku University, Aoba-yama 07, Sendai 980-8579, Japan*
[b] *Department of Chemistry, Indian Institute of Technology-Bombay, Powai, Mumbai 400076, India*
[c] *PRESTO, Japan Science and Technology, 4-1-8 Honcho Kawaguchi, Saitama 332-0012, Japan*
[d] *New Industry Creation Hatchery Center (NICHe), Tohoku University, Aoba-yama 10, Sendai 980-8579, Japan*

Received 27 October 2003; accepted 12 April 2004

Abstract

We report a theoretical study on the cyclopropane adsorption onto Cu(1 1 1) surfaces by density functional theory (DFT) and quantum chemical molecular dynamics methods. The equilibrium geometry of the physisorbed species was obtained using both periodic and cluster models by DFT methods that employ Cambridge serial total energy package (CASTEP), DMol ab initio quantum chemistry software of Accelrys' materials studio (DMol), and Amsterdam density functional (ADF) program. It was found that the adsorbate molecule was tilted towards the metal surface with one C–C bond (upwards) parallel to the surface and that the physisorption occurred via a third carbon atom pointing (downwards) towards the surface. The electronic distribution and geometrical structure of physisorbed cyclopropane were slightly deviated from its gas phase molecule. The calculated vibrational frequencies and adsorption energies are close to experimental data, confirming the reliability of our DFT results. The adsorption process was simulated using our novel tight-binding quantum chemical molecular dynamics program, 'Colors'. The calculation results indicated that both the adsorption and desorption processes of cyclopropane took place molecularly. The electron transfer and structural properties of equilibrium position obtained by 'Colors' are consistent with those by the first principles DFT methods.

Keywords: Density functional theory; Quantum chemical molecular dynamics; Cyclopropane; Copper surface; Adsorption

1. Introduction

The design of new catalysts that display higher activity, stability and selectivity is the ultimate goal in the reforming of hydrocarbons since they have enormous potentials as fuel sources and petrochemical feedstock [1,2]. In the last decades, considerable attentions have been focused on an understanding of the interactions between the hydrocarbon molecules and the transition metal surfaces that are catalytically active. This is because the reactivity of C–C and C–H bonds on metal surfaces can provide valuable information about the initial elementary reaction mechanisms and the activation modes at the molecular level. Although the surface chemistry of hydrocarbons has been examined [3], a detailed description of the adsorption processes still remains unclear especially for the adsorbates that contain three or more carbon atoms. Here addressed the activation of saturated cyclic hydrocarbons, cyclopropane (c-C_3H_6) that have served as an ideal probe molecule for hydrocarbon transformation reactions on different metal surfaces [4–6].

Chemically, c-C_3H_6 is an attractive adsorbate for several reasons: First c-C_3H_6 is a saturated molecule of both olefinic and paraffinic characters; it has a relatively weak C–C bond energy of 289 kJ mol^{-1} as compared to 347 kJ mol^{-1} for normal hydrocarbons [7,8]; secondly, the relatively high reactivity of c-C_3H_6, as a consequence of highly strained C–C bonds, results in its use as a simple probe molecule as

* Corresponding author. Tel.: +81 22 217 7233; fax: +81 22 217 7235.
E-mail address: miyamoto@aki.che.tohoku.ac.jp (A. Miyamoto).
[1] Present address: Department of Chemistry, College of Chemistry and Chemical Engineering, Inner Mongolia University, China.

1381-1169/$ – see front matter © 2004 Elsevier B.V. All rights reserved.
doi:10.1016/j.molcata.2004.04.044

compared to the straight chain alkanes. Therefore, *c*-C_3H_6 has been used for studying issues that are directing to the reaction mechanisms, reactivity and modeling on a range of metal single-crystal and supported metal catalysts [9–18]. It has been found that on the copper surfaces, *c*-C_3H_6 typically adsorbs and desorbs molecularly at low temperatures with a desorption energy of about 9 kcal/mol. Under the irradiation energy of about 10 eV, the chemical adsorption intermediates can be produced by effectively breaking C–H and C–C bond, as confirmed by the studies of the reaction of *c*-C_3H_6 with metal ion beams on the copper surfaces [19,20]. The possible dissociative adsorption species are listed in Fig. 1. It is clear that when *c*-C_3H_6 adsorbed on the copper surfaces, the physical and chemical adsorptions occur separately at different initial conditions. Thus, the knowledge of actual surface species and details of adsorption processes allow identifying the activation mechanism and interactions between cyclopropane (*c*-C_3H_6) and copper surfaces.

The activation mechanism of C–C bond in *c*-C_3H_6 has been investigated by studying the reactivity of organometallic clusters or characterizing the reactivity of a range of catalytic materials, in which the fundamental quantum chemical calculation and molecular dynamics simulation are proved to be suitable for modeling the surface chemistry of hydrocarbons and the unusual reactivity of *c*-C_3H_6 [21,22]. Quantum chemical calculations have been performed on the relationships between the reactivity and bonding properties of *c*-C_3H_6 for Rh and Ir complexes [23]. A Hartree–Fock ab initio method has also been applied to study the *c*-C_3H_6 for the copper surface using the cluster model where the molecular ring plane of adsorbate molecule is placed parallel to the surface [24]. However, some challenging problems develop when we model the adsorption process and identify the adsorption species for *c*-C_3H_6 on the copper surfaces. The adsorption takes place in an associative way and there are no dissociated surface species formed during the physisorption process, whereas the dissociated species appear under the irradiation at a power of about 10 eV. The molecular level descriptions including the electronic interaction and dynamic behaviors of the associative and dissociative adsorption are still not satisfactory to the scientific community. Thus we focus our attention on the theoretical investigation of different adsorption processes with the aim of getting a deeper understanding of the activation mechanism for *c*-C_3H_6 that is adsorbed on the metal surfaces. As a primitive and fundamental step, we started our investigation on the associative adsorption process, i.e. the physisorption process. In this paper, the optimized structures of the physisorbed *c*-C_3H_6 on Cu(1 1 1) surface are calculated by the first principles density functional theory. The electronic interaction between adsorbate and adsorbent is discussed, based on the analysis of Mulliken population. Our novel tight-binding quantum chemical molecular dynamics program, 'Colors', is employed to provide the dynamic details of the complete adsorption processes.

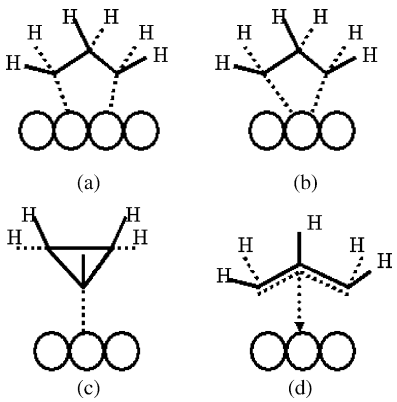

Fig. 1. The possible species when cyclopropane is adsorbed on the metal surfaces: (a) pentanuclear ring, (b) metallacyclobutane, (c) cyclopropyl (η^1-allyl) and (d) cyclopropyl (π or η^3-allyl).

2. Computational methods

A proper understanding of the activation mechanism in an adsorption system requires the accurate electronic and structural information for the interactions between adsorbate and adsorbent as well for the reliable dynamic details of the whole adsorption processes. The code 'Colors', which was developed in our laboratory, has been used to investigate these properties. For comparison, the first principles quantum chemical method of DFT [25] was also carried out to calculate the electronic and structural properties.

In DFT, the total energy, E, of the system is calculated in terms of the following expression:

$$E = V_{NN} + H' + V_{ee} + E_{ex}(\rho) + E_{corr}(\rho)$$

where V_{NN} is the nuclear–nuclear interaction; H' is the mono-electronic contribution to the total energy involving the electron–kinetic and electron–nuclear interactions; V_{ee} is the Columbic interaction between electrons; and $E_{ex}(\rho)$ and $E_{corr}(\rho)$ are the exchange and correlation energies, respectively. All terms except for the nuclear-nuclear repulsion are the functions of the electron density ρ [25]. The calculations were performed by Cambridge serial total energy package (CASTEP) [26], DMol ab initio quantum chemistry software of Accelrys' materials studio (DMol) [27], and Amsterdam density functional (ADF) program [28]. By the CASTEP program, the geometry optimization of physisorbed *c*-C_3H_6 onto Cu(1 1 1) surface is refined using a periodic model. The norm-conserving non-local pseudo-potentials are generated using the Kerker scheme with a kinetic energy cutoff at 400 eV for the plane-wave basis set expansion of wave functions. The default convergence criteria of CASTEP was applied, i.e., 0.00002 eV for the energy change per atom, 0.001 for the root-mean-square atomic displacement, and 0.05 eV/Å for the root-mean-square residual force on movable atoms. For the method of DMol, geometry optimization procedure is performed with standard parameters provided by the program. SCF density convergence,

optimization energy convergence and gradient convergence equal 0.001, 0.00001 and 0.01 a.u, respectively. Electron exchange and correlation are described by the local density approximation on the basis of the Vosko, Wilk and Nusair publications (Vosko et al., 1980) [29]. The calculations are performed with the DNP basis sets, double numerical basis sets supplemented by polarization functions. The electronic properties of the isolated c-C_3H_6 molecule as well as c-C_3H_6 adsorbed on Cu(1 1 1) surface are carried out using the ADF program with a cluster model. The calculation applies the triple-zeta basis sets that contain a polarization function with the Perdew–Wang (PW91XC) exchange and correlation potential [30] at the generalized gradient approximation (GGA) level. The inner electrons up to the core shells (1s for C; 2p for Cu) are frozen. The relativistic terms are calibrated by a combined scalar relativistic zero order regular approximation (ZORA) [31].

The 'Colors' program is based on our original tight-binding quantum chemical molecular dynamics method and can provide electronic and structural information as well as the dynamic behavior of the adsorption processes [32,33]. In 'Colors', the total energy, E, is given by the following expression:

$$E = \sum_{i=1}^{n} \tfrac{1}{2} m_i {v_i}^2 + \sum_{k=1}^{\mathrm{occ}} \varepsilon_k + \sum \sum_{i>j} \frac{Z_i Z_j e^2}{R_{ij}} + \sum \sum_{i>j} E_{\mathrm{rep}}(R_{ij}) \quad (1)$$

where the first, second, third, and fourth terms represent the kinetic energy of nucleus, the summation of the eigenvalues of all occupied orbitals (orbital energy of valence electrons), the Columbic interaction energy, and the short-range exchange-repulsion interaction energy, respectively. Here, m and v are mass and velocity of the atoms; Z_i and Z_j are the charges of the atoms; e is the elementary electric charge; and R_{ij} is the internuclear distance. The short-range exchange-repulsion term, E_{rep} (R_{ij}), is given by:

$$E_{\mathrm{rep}}(R_{ij}) = b_{ij} \exp\left[\frac{a_{ij} - R_{ij}}{b_{ij}}\right] \quad (2)$$

where a_{ij} and b_{ij} represent the sum of the size and stiffness of atoms, i and j, respectively. The force can be expressed as follows:

$$F_i = \sum_{j\neq i}^{n} \sum_{k=1}^{\mathrm{occ}} C_k^{\mathrm{T}} \left(\frac{\partial H}{\partial R_{ij}}\right) C_k + \sum_{j\neq i}^{n} \sum_{k=1}^{\mathrm{occ}} \varepsilon_k C_k^{\mathrm{T}} \left(\frac{\partial S}{\partial R_{ij}}\right) C_k - \sum_{j\neq i}^{n} \frac{Z_i Z_j e^2}{R_{ij}^2} + \sum_{j\neq i}^{n} \frac{\partial E_{\mathrm{rep}}(R_{ij})}{\partial R_{ij}} \quad (3)$$

where H is the Hamiltonian matrix, S the overlap integral matrix, C the eigenvector matrix, and C^{T} the transformation matrix of the eigenvector matrix C. Based on the improved Wolfsberg–Helmholz formula by Anderson [34] and Calzaferri et al. [35], we employed the following corrected distance-dependent expression K for off-diagonal terms of the Hamiltonian H_{rs}:

$$H_{\mathrm{rs}} = \tfrac{1}{2} K_{\mathrm{rs}} (H_{\mathrm{rr}} + H_{\mathrm{ss}}) S_{\mathrm{rs}} \quad (4)$$

$$K_{\mathrm{rs}} = 1 + (\kappa_{\mathrm{rs}} + \Delta^2 - \Delta^4 \kappa_{\mathrm{rs}}) \exp\left[-\delta_{\mathrm{rs}}(R_{ij} - d_0)\right] \quad (5)$$

$$\Delta = \frac{H_{\mathrm{rr}} - H_{\mathrm{ss}}}{H_{\mathrm{rr}} + H_{\mathrm{ss}}} \quad (6)$$

where H_{rr} is the diagonal term of Hamiltonian matrix and is equal to the first ionization energy of each atomic orbital and d_0 is the sum of the orbital radii.

In order to realize the high accuracy, the parameters are established by our new parameterization procedure based on the first principles density functional theory calculations. The single or double-ξ Slater-type orbital with a charge-dependent Slater exponent is used to describe atomic orbitals in 'Colors'. The charge-dependent exponent coefficients for 'Colors' are determined by fitting the ADF results of radial electron density distributions. As is seen from Fig. 2, the agreement is almost complete except for the inner nodes that do not affect the chemical bonding. The ionization potentials used for the diagonal term of Hamiltonian matrix are also fitted to the ADF results. Fig. 3 shows the ionization potentials of hydrogen, carbon, and copper for the 'Colors' program. The agreement with the ADF and experiments is almost complete. The parameters κ_{rs} and δ_{rs} in the tight-binding Hamiltonian and the parameters a_{ij} and b_{ij} in the short-range exchange-repulsion term are determined so as to satisfy the bond lengths, binding energies, frequencies of diatomic molecules, and potential energy curves obtained by ADF. Fig. 4 shows the typical potential curve of diatomic molecules used in this work such as C–H, Cu–Cu, Cu–C and C–C. It is clear that the energy curves obtained by both the ADF and 'Colors' programs are nearly identical. Further details regarding the process of our parameterization can be seen elsewhere [32]. The reliability of the 'Colors' method has been confirmed in refs. [33,36,37]. In addition, the calculations performed on different systems using 'Colors' indicate that the method is over 5000 times faster than the traditional first principles quantum chemical molecular dynamics calculations. In this work, quantum chemical molecular dynamics calculations were carried out to simulate the experiments in vacuum under ambient pressure and temperature conditions by using our 'Colors' code. The Verlet algorithm was used for the calculation of atomic motions. Temperature is controlled by scaling the atom velocities under three-dimensional periodic boundary conditions. The calculations are performed with a time step of 2 fs for a total time of 4000 fs at 298 K.

For the visualization of the CASTEP and DMol results, viz., geometrical structures, we utilized computer graphics molecular visualization program CERIUS2 [38]. In the case of ADF, we employed MOLEKEL4.1 for the visualization of molecular orbital and optimized structures [39]. For

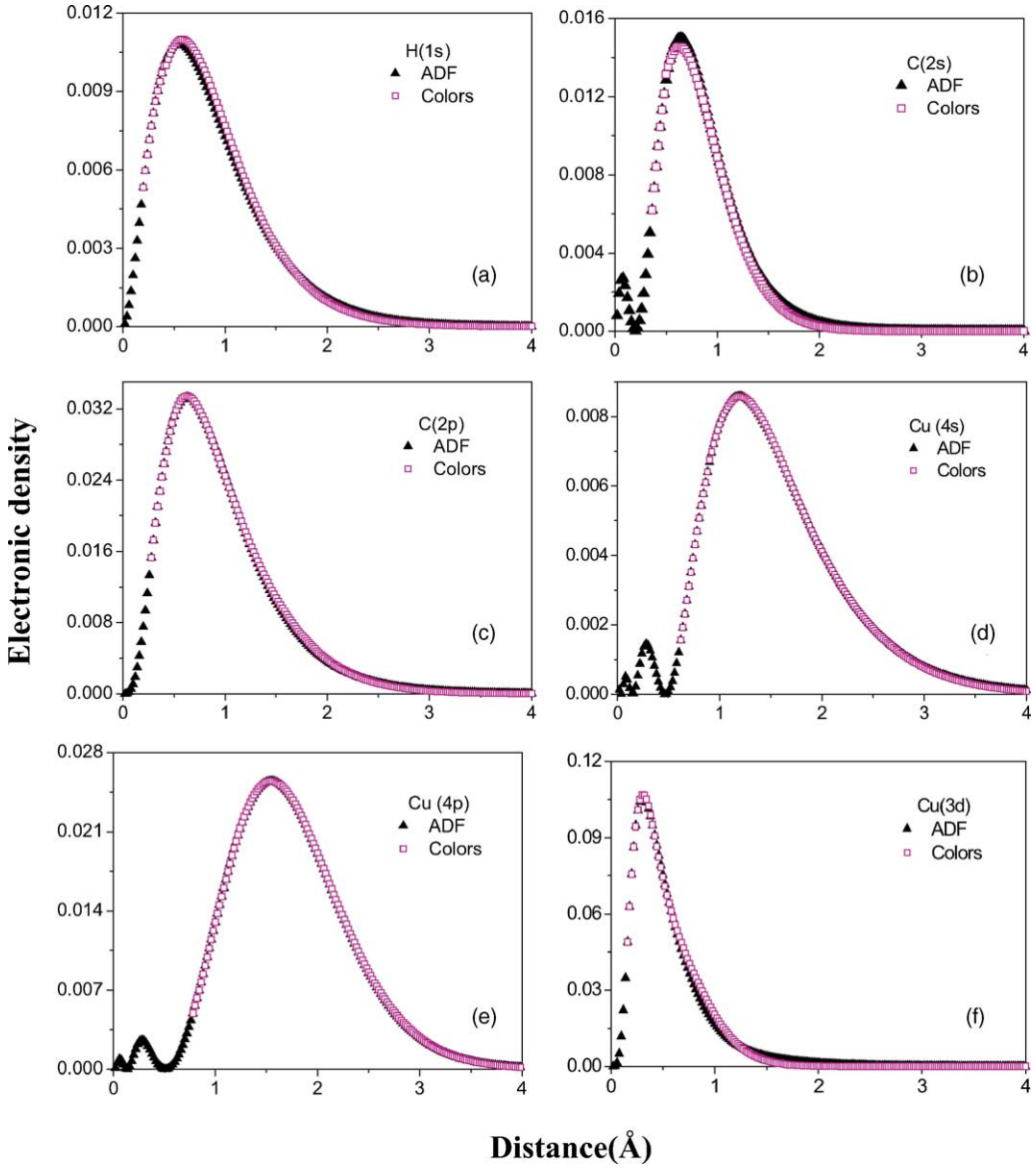

Fig. 2. Electron density distribution of various atomic orbitals calculated by ADF and 'Colors': (a) H(1s), (b) C(2s), (c) C(2p), (d) Cu(4s), (e) Cu(4p) and (f) Cu(3d).

three-dimensional visualization of quantum chemical molecular dynamics results obtained by 'Colors', we used a computer graphics code New-RYUGA, which was developed in our laboratory [40].

3. Results and discussion

Fig. 5 depicts the optimized structure of *c*-C_3H_6. Table 1 summarizes the calculated geometrical data of *c*-C_3H_6 employing ADF, DMol, CASTEP, and 'Colors'. For the 'Colors' program, a dynamic simulated annealing method was used by setting up a temperature $T = 300$–1 K to get the stable equilibrium state, whereas for other methods the optimized structures are obtained by minimizing the total

Table 1
The bond lengths (in Å) of gas phase *c*-C_3H_6 by ADF, CASTEP, DMol and 'Colors'

Bond	Methods				Experimental [41]
	ADF	CASTEP	'Colors'	DMol	
C2–C3	1.511	1.511	1.526	1.509	1.510
C1–C2	1.511	1.511	1.526	1.509	1.510
C1–C3	1.511	1.511	1.526	1.510	1.510
C1–H	1.088	1.090	1.118	1.089	1.089
C1–H	1.088	1.090	1.118	1.089	1.089
C2–H	1.088	1.090	1.118	1.089	1.089
C2–H	1.088	1.090	1.118	1.089	1.089
C3–H	1.088	1.090	1.118	1.089	1.089
C3–H	1.088	1.090	1.118	1.089	1.089

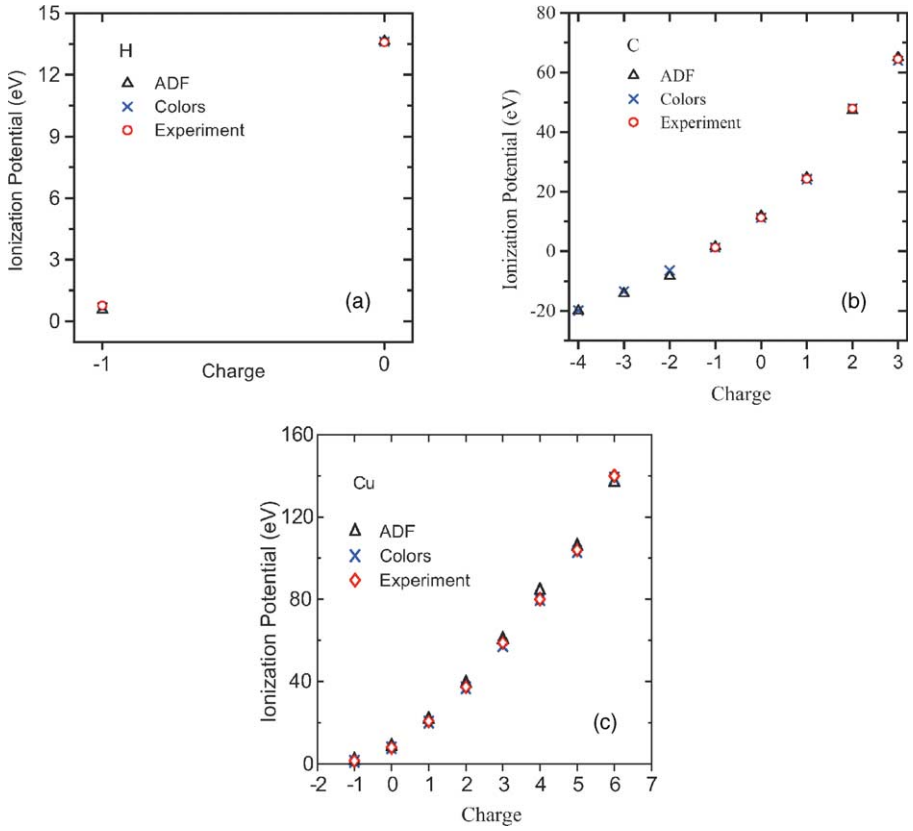

Fig. 3. Ionization potentials for various atoms and ions by ADF and 'Colors': (a) hydrogen, (b) carbon and (c) copper.

energy. It is known that the symmetry of *c*-C_3H_6 remains D_{3h} point group and the calculated structural parameters are in good agreement with each other and also with the literature data [41].

In order to get the equilibrium geometry of *c*-C_3H_6 adsorbed on Cu(1 1 1) surface, we perform a CASTEP full optimized calculation for periodic metal crystal. For this purpose, we assume three different periodic models as initial structures to represent the different adsorption manners, i.e., the molecular plane of *c*-C_3H_6 is placed parallel to the copper surface (Fig. 6a), perpendicular to the surface with one C–C bond pointing upwards (Fig. 6b) or downwards (Fig. 6c) to the copper surface. The periodic boundary conditions with 2 × 2 super cell are imposed during calculation, the experimental unit cell parameter of copper crystal ($a = 7.2294$ Å and $b = 7.2294$ Å) are used, and the *c*-axis is set sufficiently large so as to eliminate the interactions, if any, between the periodic images in the surface adsorption processes. For the initial models of Fig. 6a,b, the final equilibrium structures have a typical geometry as shown in Fig. 7a, i.e., the adsorbate molecule was tilted towards the surface with one bond of C–C parallel (upward) to the surface of copper. This tilted adsorption configuration resembles that as is indicated experimentally for *c*-C_3H_6 on other metal surfaces [42–44]. Therefore, to further study the electronic properties by ADF, the cluster models will be fetched from this tilted equilibrium geometry. However, for the initial adsorption manner given in Fig. 6c, the convergence results cannot be reached. This is however reasonable because the initial structure of this model is far from the equilibrium geometry if we assure that the tilted adsorbate with one bond upward to the surface is of actually minimum-energy adsorption geometry. The same calculations are performed by the periodic DMol method. The optimized bond lengths and Mulliken charges of *c*-C_3H_6 are shown in Table 2. The geometrical structure is very similar to that obtained by CASTEP (Fig. 7). The slight differences between two methods are that the adsorbate is not so tilted to the surface and there is a little longer distance between adsorbate and surface in DMol than in CASTEP.

The calculation of cluster model is carried out by ADF for the comparison with the further investigation on the chemical adsorption processes in future, which is related to the electronically excited states and can be handled by the ADF response module [28]. An isolated cluster fetched from the results of CASTEP optimized geometry is subjected to the calculation using the ADF program. In this study, two different cluster sizes are employed for the adsorption of *c*-C_3H_6 onto Cu(1 1 1) substrate. The initial model I is chosen for a cluster that includes one *c*-C_3H_6 as adsorbate and 16 copper atoms as adsorbent and is distributed in two layers with 10 Cu atoms on the top layer and six Cu atoms in the bottom layer (see Fig. 8a). To confirm that the adsorbent with 16 copper atoms is big enough to simulate the monolayer

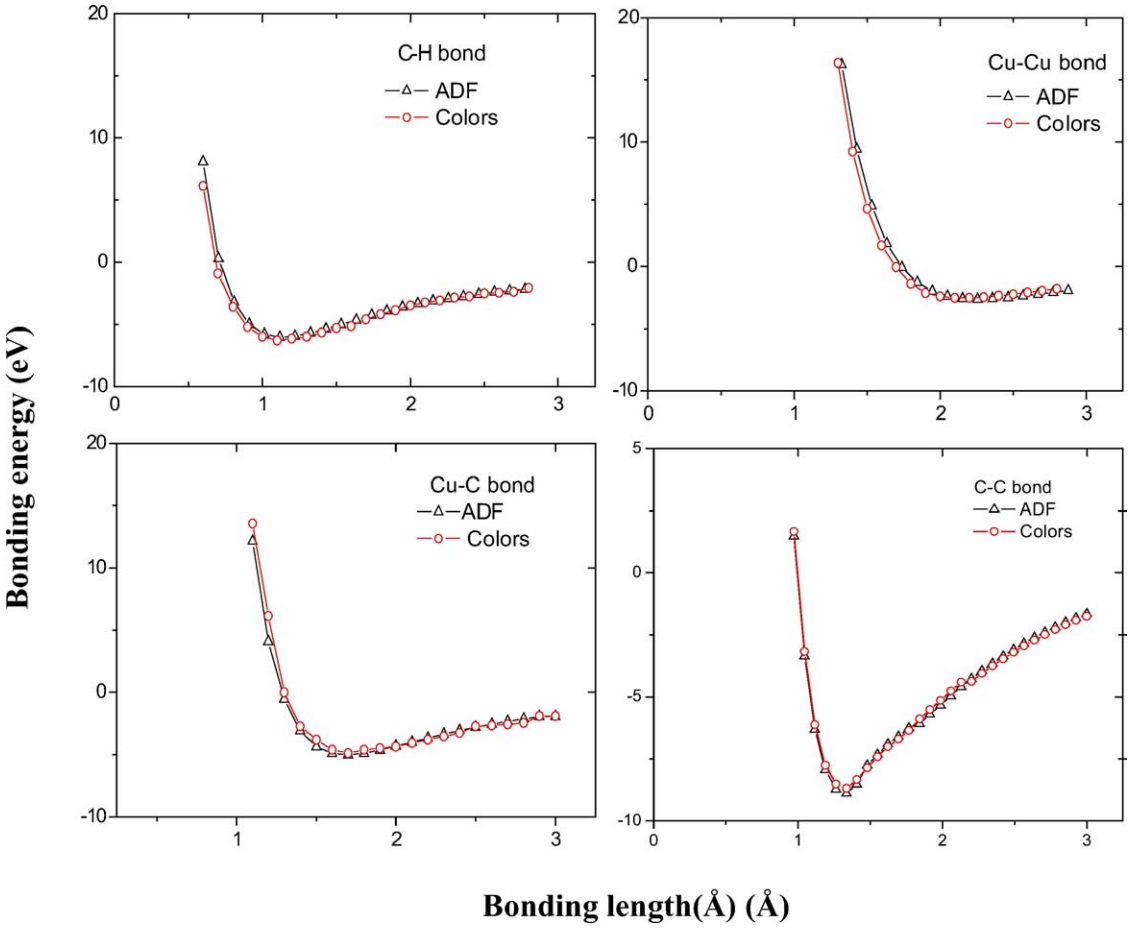

Fig. 4. Potential curve of the small molecule CH, Cu_2, CuC and C_2 by ADF and 'Colors'.

adsorption, we also employ model II in which the numbers of Cu atoms in adsorbent is increased to 32 with an equal distribution of 16 in each layer (see Fig. 8b). The respective final optimized structures of *c*-C_3H_6 adsorption on the copper surface are illustrated in Fig. 9. It can be found that very similar structures have been obtained using these two models. The adsorption geometries show that one carbon atom (C1) is near to the copper surface while the entire molecular ring is not parallel to the surface. This tilted adsorption configuration is consistent with the results obtained by the periodic density functional methods of CASTEP and DMol. The calculation results of bond lengths, overlap populations, and Mulliken charges of adsorbate are listed in Tables 2–4. The geometry and distribution of electrons are a little different for the molecules at adsorbed states and those in gas phase. As is seen from Table 2, the nearest distance of carbon and copper is 3.408 Å (Fig. 9a) and 3.509 Å (Fig. 9b). The slightly longer distances between copper and carbon indicate that there are no bonds formed between copper and carbon in these two structures. This has been proved by the results of the overlap populations and a near zero values of Cu–C bonds (see Table 3). Further, it can be seen from Table 2 that the net charge of adsorbate molecule is only −0.090 and −0.092 in these two geometries, which means that there is slight electron transfer from copper to *c*-C_3H_6 in these two geometries. The interactions between adsorbate and adsorbent are therefore very weak. The Mulliken populations of carbon atom (C1) that is closer to the copper surface and two hydrogen atoms bonded to C1 are quite different from other two carbon atoms (C2 and C3) and other four hydrogen atoms (Table 4). Moreover, the Mulliken populations of C2 and C3 are very close to the values of *c*-C_3H_6 in gas-phase. Therefore it can be concluded that the weak in-

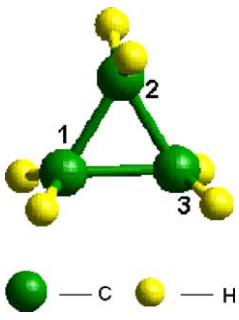

Fig. 5. The optimized structure of *c*-C_3H_6.

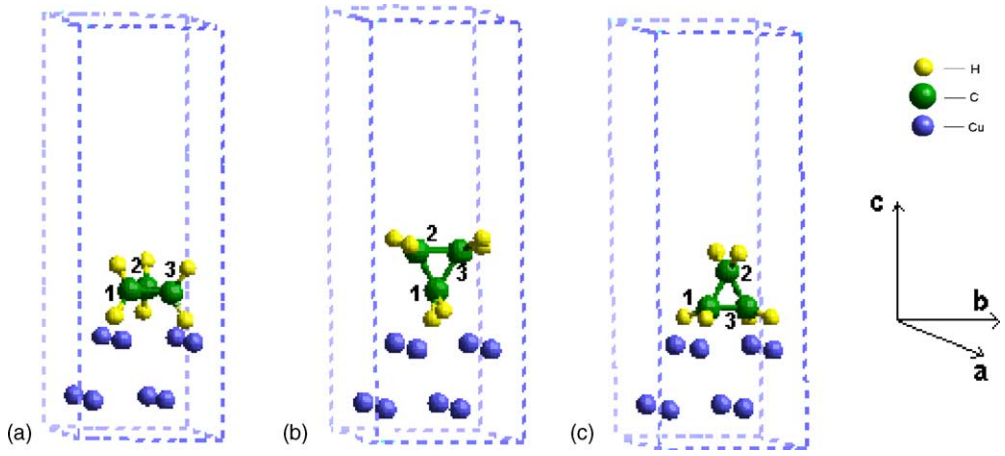

Fig. 6. The initial periodic models: (a) *c*-C_3H_6 parallels to the copper surface, (b) *c*-C_3H_6 vertical to the copper surface with one bond of C–C upward to the surface, and (c) *c*-C_3H_6 vertical to the copper surface with one bond of C–C downward to the surface.

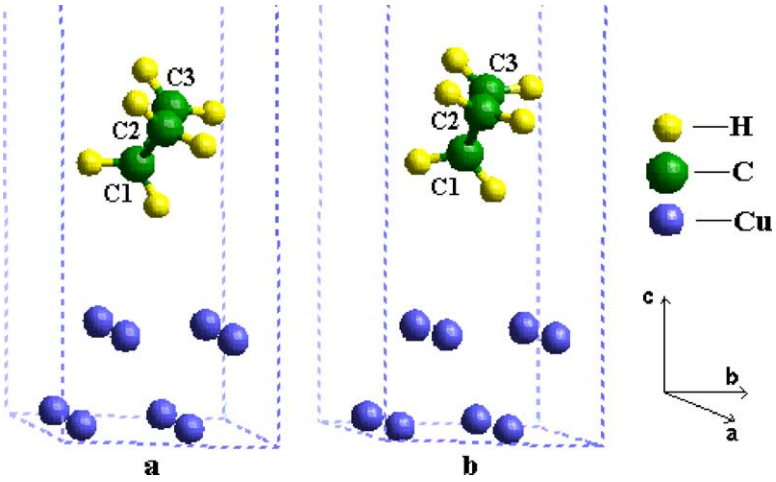

Fig. 7. The final optimized results of *c*-C_3H_6 adsorption on the copper surface by CASTEP and DMol. (a) The result by CASTEP, (b) the result by DMol.

Table 2
The bond lengths (in Å) and net charge of the *c*-C_3H_6 using different adsorption models

Bond	CASTEP	DMol	ADF		'Colors'
	Geometry in Fig. 7a	Geometry in Fig. 7b	Geometry in Fig. 9a	Geometry in Fig. 9b	Geometry in Fig. 10b
C2–C3	1.513	1.508	1.507	1.506	1.523
C1–C2	1.513	1.510	1.511	1.514	1.537
C1–C3	1.511	1.512	1.510	1.510	1.536
C1–H	1.088	1.090	1.093	1.090	1.145
C1–H	1.088	1.090	1.093	1.090	1.145
C2–H	1.088	1.089	1.089	1.089	1.133
C2–H	1.088	1.089	1.088	1.089	1.133
C3–H	1.050	1.088	1.089	1.088	1.098
C3–H	1.050	1.088	1.089	1.088	1.098
C–Cu	3.309	4.082	3.408	3.509	3.484
Cu–Cu	2.556	2.556	2.556	2.556	2.556
Net charge	–	−0.020	−0.090	−0.092	−0.045

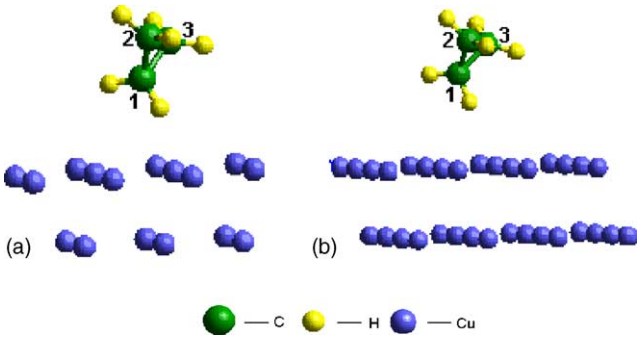

Fig. 8. The initial cluster models (a) *c*-C_3H_6 as adsorbate and 16 copper atoms as adsorbent and (b) *c*-C_3H_6 as adsorbate and 32 copper atoms as adsorbent.

Table 3
The atom–atom overlap populations of the adsorption systems using different models and in gas phase *c*-C_3H_6

Atoms	Geometry in Fig. 9a	Geometry in Fig. 9b	Gas-phase
C2–C3	0.2666	0.2643	0.2562
C1–C2	0.2293	0.2277	0.2562
C1–C3	0.2293	0.2244	0.2562
C1–H	0.4012	0.4157	0.4336
C1–H	0.4041	0.4100	0.4336
C2–H	0.4345	0.4346	0.4336
C2–H	0.4372	0.4345	0.4336
C3–H	0.4362	0.4380	0.4336
C3–H	0.4365	0.4368	0.4336
C–Cu	0.0098	0.0084	–

teraction mainly occurs between metal surface and the carbon atom that is closer to the metal surface (C1). As a consequence, the structure of adsorbate does not belong to the D_{3h} symmetry as it is in free gas-phase molecules.

The reliability of our results can be confirmed through the vibration frequencies. The vibration frequencies calculated by ADF for cluster model I (shown in Fig. 9a) are listed in Table 5. The five assigned main loss peaks exhibit the

Table 4
The Mulliken populations of the adsorption systems of different models and in gas phase *c*-C_3H_6

Atom	Orbital	ADF		Gas-phase
		Geometry in Fig. 9a	Geometry in Fig. 9b	
C1	2s	1.05	1.07	1.05
	2p	2.49	2.49	2.66
C2	2s	1.07	1.08	1.05
	2p	2.66	2.66	2.66
C3	2s	1.08	1.08	1.05
	2p	2.67	2.67	2.66
H (C1)	1s	1.00	0.99	1.04
H (C1)	1s	0.96	0.96	1.04
H (C2)	1s	1.05	1.05	1.04
H (C2)	1s	1.05	1.05	1.04
H (C3)	1s	1.05	1.05	1.04
H (C3)	1s	1.05	1.06	1.04

typical structures of cyclic-C_3 species [45,16]. The similarities between the gas phase and adsorbed phase of adsorbate molecule proved that there are no strong interactions between *c*-C_3H_6 and copper surface during the physical adsorption processes. Our results fit well with the HREELS experimental results except for an increase in the numbers of the vibration models which are assigned to the loss of local symmetry as induced by the interactions between cyclic-C_3H_6 and copper surface. However, it should be noted that the frequency calculation for the cluster model II (shown in Fig. 9b) has not been analyzed in this work owing to the technical difficulty for the large systems.

The adsorption energy representing the degree of interaction between adsorbate and adsorbent during adsorption processes is also derived according to the following equation:

$$E_{ad} = E_{metal_{+adsorbate}} - (E_{metal} + E_{adsorbate})$$

where E_{metal}, $E_{adsorbate}$ and $E_{metal_{+adsorbate}}$ represent the total energies of copper cluster, gas phase *c*-C_3H_6 molecule and

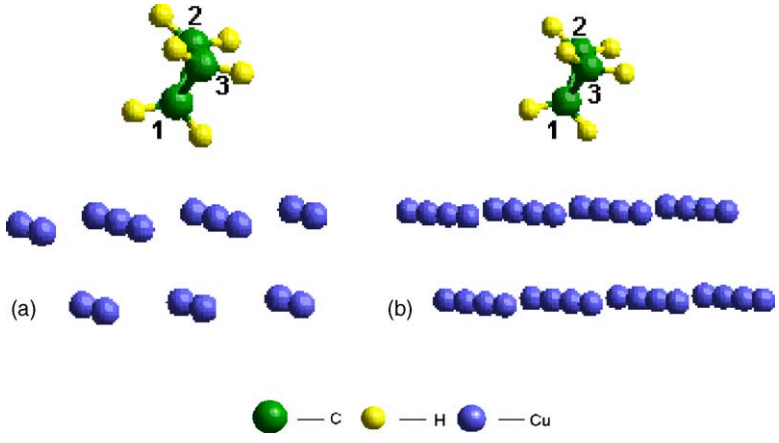

Fig. 9. The optimized structures by ADF. (a) The result from the initial model of Fig. 8a. (b) The result from the initial model of Fig. 8b.

Table 5
The data of vibrational frequency (cm^{-1}) for the adsorption systems at physical adsorption (geometry in Fig. 9a) and in gas phase c-C_3H_6

Vibrational model	Calculated (this work)		Experimental [16,45]	
	Geometry in Fig. 9a	Gas-phase	Physial adsorption	Gas-phase
CH stretching	3007–3161	3062–3161	3064	3024–3102
CH_2 deformation	1409–1458	1424–1472	1451	1438–1479
Ring breathing	1019–1194	1179	1177	1188
Asymmetric ring deformation	987–979	1013	1032	1028
Symmetric ring deformation	857–879	861	839	867

Table 6
The adsorption energies (E_{ad}) by CASTEP, DMol and ADF

Method	Model	E_{ad} (kcal/mol)
CASTEP	Structure in Fig. 7a	19.28
DMol	Structure in Fig. 7a	1.09
ADF	Structure in Fig. 9a	6.1
	Structure in Fig. 9b	7.4
Experimental [19]		9.0

the adsorbed system (metal + adsorbate), respectively. The results by the DFT methods of CASTEP, DMol and ADF are listed in Table 6. The cluster model of ADF yields the adsorption energy of 6.1 kcal/mol for model I (in Fig. 9a) and 7.4 kcal/mol for model II (in Fig. 9b). These calculation results are in agreement with that of 9.0 kcal/mol as determined experimentally [19]. The very small value produced by DMol is consistent with the longer distance between adsorbate and metal surface. Obviously, the small adsorption energies are obtained by these methods, which indicate weak physisorption of c-C_3H_6 on the copper surfaces.

Finally, the dynamic details during the evolution of adsorption process are derived using our tight-binding quantum chemical molecular dynamics code 'Colors'. The reliability of this program has been documented well in literature [36,37]. We set up the initial model with similar optimized structure to those obtained by the periodic model of DFT (see Fig. 7), while the unit cell dimension is doubled, i.e. from 7.2294 Å × 7.2294 Å to 14.4588 Å × 14.4588 Å, to well mimic the practical metal surface owing to the convenience of large system calculation by the 'Colors' code. Fig. 10 presents the geometries of the adsorbate molecule on the adsorbent at different time intervals. It can be seen that at the initial stages, the adsorbate molecule moves towards the surface, but as the time increases it moves away from the surface. The plot of distance versus time (Fig. 11) shows that the distance between carbon (C1) and copper (nearest to the adsorbate) is continuously changing with the time. It is also obvious that the distance between carbon and carbon does not change greatly with the time; however the distance of carbon and copper become shorter at the beginning, then reaching a minimum distance at a time of 1200 fs. After that time, it becomes longer with a further increase in time, which suggests that the desorption may also occur associatively. The value of electrons transferring at the geometrical structure where the adsorbate is nearest to the copper surface was obtained by analyzing the Mulliken charge. There is −0.045 electrons transfer from metal to c-C_3H_6 (Table 2), showing a weak interaction between the copper surface and adsorbent molecule. This value is consistent with those obtained by DFT methods (Table 2). The geometrical data of adsorbate in this case is also listed in Table 2. They are close to those obtained by the ADF and DMol programs, confirming the reliability of our 'Colors' program.

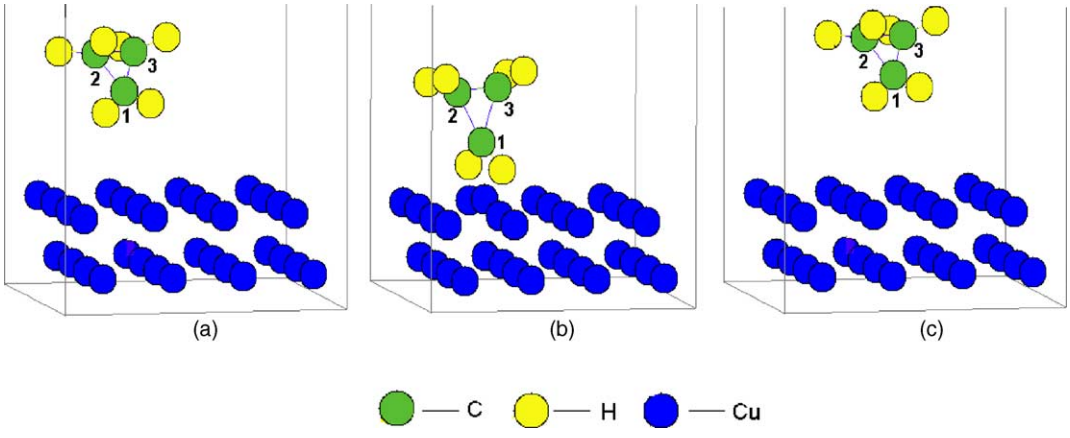

Fig. 10. Geometries of the adsorbed c-C_3H_6 on copper surface at different time internals of (a) 0 fs, (b) 1200 fs and (c) 4000 fs by 'Colors'.

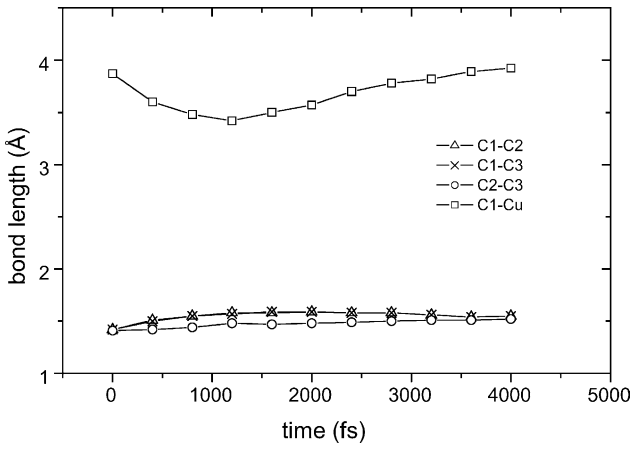

Fig. 11. Evolution of the bond distance during the adsorption process by 'Colors'.

4. Conclusion

The geometries, electron transfer and physisorption behavior of *c*-C_3H_6 on Cu(1 1 1) surface were theoretically studied using our novel tight-binding quantum chemical molecular dynamics program, 'Colors'. Our calculations showed that the *c*-C_3H_6 adsorbs molecularly on copper surface with one C–C bond parallel (upward) to the surface while the entire molecule tilting to the surface. A very weak electron transfer and the longer distance between adsorbate and copper surface indicated the absence of strong interaction. The adsorbate molecule moved to the surface and reached a nearest position at the distance of 3.42 Å from the copper surface. On the other hand, the adsorbate molecules moved away from the adsorbent with an increase in the adsorption time. The structural and electronic properties at adsorption equilibrium were also calculated by the first principles density functional theory with periodic and cluster models using the CASTEP, DMol and ADF programs. The calculated vibrational frequencies and adsorption energies are in good agreement with the experimental data. Consistently, the results indicated the tilted adsorbed geometrical structure and a weak interaction between adsorbate and adsorbent.

References

[1] R.W. Verhoef, D. Kelly, C.B. Mullins, W.H. Weinberg, Surf. Sci. 325 (1995) 93.
[2] D.F. Johnson, W.H. Weinberg, J. Chem. Phys. 103 (1995) 5833.
[3] F. Zaera, Chem. Rev. 95 (1995) 2651.
[4] J. Schwank, J.Y. Lee Jr., J.G. Goodwin, J. Catal. 108 (1987) 495.
[5] M.W. Simon, C.O. Bennett, S.L. Suib, J. Catal. 100 (1994) 148.
[6] R. Brown, C. Kemball, J. Chem. Soc. Faraday Trans. 86 (1990) 3815.
[7] J.G. Hamilton, W.E. Palke, J. Am. Chem. Soc. 115 (1993) 4159.
[8] J. Gauss, D. Cremer, J.F. Stanton, J. Phys. Chem. A 104 (2000) 1319.
[9] A.T. Capitano, J.L. Gland, Langmuir 14 (1998) 1345.
[10] C.J. Hagedorn, M.J. Weiss, T.W. Kim, W.H. Weinberg, J. Am. Chem. Soc. 123 (2001) 929.
[11] T.A. Jachimowski, W.H. Weinberg, Surf. Sci. 370 (1997) 71.
[12] P. Lenz-Solomun, D.W. Goodman, Langmuir 10 (1994) 172.
[13] K.A. Son, J.L. Gland, J. Am. Chem. Soc. 118 (1996) 10505.
[14] A.J. Franz, J.T. Ranney, J.L. Gland, S.R. Bare, Surf. Sci. 374 (1997) 162.
[15] R. Martel, A. Rochefort, P.H. McBreen, J. Am. Chem. Soc. 116 (1994) 5965.
[16] R. Martel, A. Rochefort, P.H. McBreen, J. Am. Chem. Soc. 119 (1997) 7881.
[17] Y.L. Tsai, B.E. Koal, J. Phys. Chem. B 101 (1997) 4781.
[18] P.D. Szuromi, J.R. Engstrom, W.H. Weinberg, J. Chem. Phys. 80 (1984) 508.
[19] R. Martel, A. Rochefort, P.H. McBreen, J. Am. Chem. Soc. 120 (1998) 2421.
[20] R. Martel, P.H. McBreen, J. Phys. Chem. B 101 (1997) 4966.
[21] K. Ohe, H. Matsuda, T. Morimoto, S. Ogoshi, N. Chatani, S. Murai, J. Am. Chem. Soc. 116 (1994) 4125.
[22] M.J.S. Dewar, J. Am. Chem. Soc. 106 (1984) 669.
[23] W.E. Charles, H.B. Michael, Organometallics 20 (2001) 5606.
[24] C. Woll, K. Weiss, P.S. Bagus, Chem. Phys. Lett. 332 (2000) 553.
[25] D.R.M. Reizler, E.K.U. Gross, Density Functional Theory: An Approach to the Quantum Many-Body Problem, Springer-Verlag, Berlin, 1990.
[26] L.C. Ciacchi, W. Pompe, A. De Vita, J. Phys. Chem. B 107 (2003) 1755.
[27] B. Delley, J. Chem. Phys. 113 (2000) 7756.
[28] G. te Velde, F.M. Bickelhaupt, E.J. Baerends, C.F. Guerra, S.J.A. van Gisbergen, J.G. Snijders, T. Ziegler, J. Comput. Chem. 22 (2001) 931.
[29] S.H. Vosko, L. Wilk, M. Nusair, Can. J. Phys. 58 (1980) 1200.
[30] J.P. Perdew, J. A Chevary, S.H. Vosko, K.A. Jackson, M.R. Pederson, D.J. Singh, C. Fiolhais, Phys. Rev. B 46 (1992) 6671.
[31] E.V. Lenthe, A.E. Ehlers, E.J. Baerends, J. Chem. Phys. 110 (1999) 8943.
[32] T. Yokosuka, H. Kurokawa, S. Takami, M. Kubo, A. Miyamoto, A. Imamura, Jpn. J. Appl. Phys. 41 (2002) 2410.
[33] M. Elanany, P. Selvam, T. Yokosuka, S. Takami, M. Kubo, A. Imamura, A. Miyamoto, J. Phys. Chem. B 107 (2003) 1518.
[34] A.B. Anderson, J. Chem. Phys. 62 (1975) 1187.
[35] G. Calzaferri, L. Forss, I. Kamber, J. Phys. Chem. 93 (1989) 5366.
[36] Y. Luo, P. Selvam, Y. Ito, S. Takami, M. Kubo, A. Imamura, A. Miyamoto, Organometallics 22 (2003) 2184.
[37] K. Sasata, T. Yokosuka, H. Kurokawa, S. Takami, M. Kubo, A. Imamura, T. Shinmura, M. Kanoh, P. Selvam, A. Miyamoto, Jpn. J. Appl. Phys. 42 (2003) 1859.
[38] Cerius^2 Tutorials—Materials Science, Molecular Simulations Inc., San Diego, 1997.
[39] S. Portmann, H.P. Luthi, Chimica 54 (2000) 766.
[40] R. Miura, H. Yamano, R. Yamauchi, M. Katagiri, M. Kubo, R. Vetrivel, A. Miyamoto, Catal. Today 23 (1995) 409.
[41] F. Dubnikova, A. Lifshitz, J. Phys. Chem. A 102 (1998) 3299.
[42] A.T. Capitano, A.M. Gabelnick, J.L. Gland, J. Phys. Chem. B 104 (2000) 3337.
[43] F.M. Hoffmann, T.E. Felter, W.H. Weinberg, J. Chem. Phys. 76 (1982) 3799.
[44] F.M. Hoffmann, T.E. Felter, P.A. Thiel, W.H. Weinberg, Surf. Sci. 130 (1983) 173.
[45] X.J. Wang, S. Takami, M. Kubo, A. Miyamoto, Chem. Phys. 279 (2002) 7.